Experimental Investigation on the Internal Clearance Induced Vibrations of Tapered Roller Bearings for Condition Monitoring

Zewen Zhou[1], Bingyan Chen[1,2], Fengshou Gu[1(✉)], Rongfeng Deng[1], Yubin Lin[1], and Yousif Muhamedsalih[1]

[1] Centre for Efficiency and Performance Engineering, University of Huddersfield, Huddersfield HD1 3DH, UK
`{zewen.zhou,f.gu}@hud.ac.uk`

[2] State Key Laboratory of Traction Power, Southwest Jiaotong University, Chengdu 610031, China

Abstract. In this study, the influence of internal clearance on vibration characteristics of tapered roller bearings (TRBs) was investigated for improving the accuracy of bearing condition monitoring which includes identifying lubricity and incipient wear. The experiments of a healthy TRB were conducted successively under three rotational speeds and four clearance conditions. The root mean square, FFT spectrum and envelope analysis were used to analyze the vibration signals. The experimental results show that the internal clearance will cause the increase of the vibration of the TRB and the appearance of the ball pass frequency of the outer race (BPFO). Moreover, the clearance will cause a deviation between the actual value of BPFO and the theoretical value, and the larger the clearance, the larger the actual BPFO. The results provide an important reference for accurate quantitative diagnosis of TRB clearances.

Keywords: Tapered roller bearings · Internal clearance · Characteristic frequency deviation · Envelope analysis · Condition monitoring

1 Introduction

Rolling bearings are key components of rotating machinery, including deep groove ball bearings, cylindrical roller bearings, tapered roller bearings (TRBs), etc. Rolling bearings exhibit good performance under combined thrust loads and medium to high speeds. Especially, TRBs are extensively used in wind turbines, helicopters, high-speed trains [1], etc. During long-term service, the rolling bearings inevitably suffer from poor lubrication and surface wear. The internal clearance reserved during assembly increases accordingly, which will cause unpredictable vibrations and affect the system's operating performance. In recent years, a variety of signal processing methods have been developed for bearing condition monitoring, such as envelope analysis [2, 3], modulation signal bispectrum [4], cyclic spectral analysis [5, 6], envelope ensemble average [7], phase

space warping [8], stochastic resonance [9]. However, most of these studies focus on localised faults rather than clearance changes due to mounting or frictional wear.

The internal clearances of the rolling bearings, including radial and axial clearance, have been the research focus for a long time. Researchers have investigated the non-linear dynamics caused by radial clearance in bearings, such as instability, chaotic bifurcation and other complex phenomena [10, 11]. However, only fewer studies have been found to focus on precise diagnosis and quantitative assessment of clearance, abnormal friction and light wear of the rolling bearing. Recently, Wang et al. [12] established a dynamic model to investigate the vibration characteristics of groove ball bearing with radial clearance. Xu et al. [13] proposed a vibration model with six degrees of freedom and concluded that radial clearance will cause the ball pass frequency of the outer race. Accordingly, Xu et al. [14] studied the effects of radial clearance and radial loads on the vibration amplitude of the rotor-bearing system.

In industrial applications, single-row tapered roller bearings are usually assembled into double-row bearings for greater load-carrying capacity [15]. Appropriate axial clearance or preload is not only necessary for the normal operation of TRBs, but also conducive to improving the support stiffness and operating accuracy of TRBs. Therefore, quantitative diagnosis and accurate online monitoring of the internal clearance are of great significance for industrial equipment. As mentioned above, most research works mainly concentrate on deep groove bearings and cylindrical roller bearings. Few scholars have studied the monitoring and diagnosis of TRB clearance in-depth, to the author's best knowledge, mainly due to the complex structure of TRB.

To fill in the gap, a TRB test rig was established (Fig. 1), and a series of experiments were carried out on TRBs with four different internal clearances, in which three rotational speeds and two load conditions were considered. The influences of clearance size and shaft rotational speed on the bearing characteristic frequency shift and root mean square (RMS) are studied. The results provide an experimental reference for accurate diagnosis of the TRB clearance size.
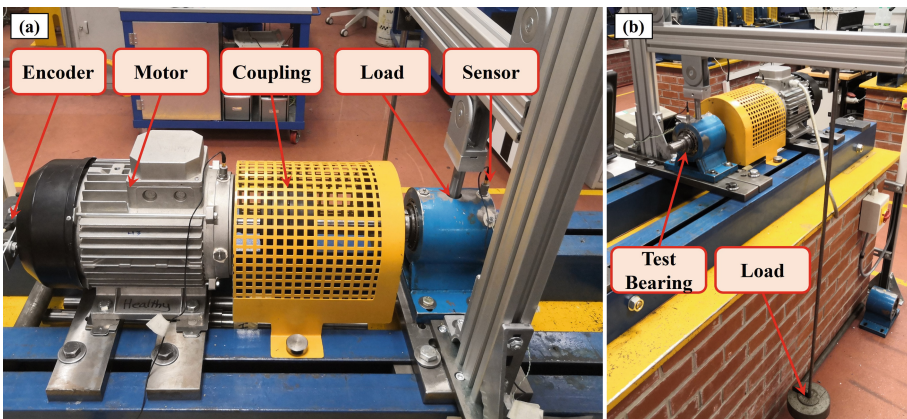

Fig. 1. (a) Tapered roller bearing test rig, (b) test bearing and loading device.

2 Description of the Experiment

2.1 Experimental Setup

To investigate the effect of internal clearance on the vibration characteristics of TRBs, a TRB test rig was designed. Figure 1a displays the main components of the TRB test bench, including a drive motor, coupling, main shaft, bearing pedestal and support bearing, etc. The test TRB is located at the end away from the drive motor. Radial loads can be set using the lever mechanism as shown in Fig. 1b. A vibration acceleration sensor is installed above the bearing seat to collect the vibration acceleration signal of the test bearing with a sampling frequency of 96 kHz. Data acquisition was performed at a constant rotational speed and the acceleration signal was collected for 45 s in each experimental condition.

2.2 Clearance Setting

The internal clearance of TRB is set by using shims of different thicknesses, as shown in Fig. 2. The setting method of the internal clearance of the TRB is described as follows: First, a shim with a certain thickness is inserted between the TRB and the fastening nut. Next, tighten the nut and set a marker position. Then, loosen the nut and remove the shim. Finally, tighten the nut to the marked position.

Fig. 2. Schematic diagram of the clearance setting.

2.3 Bearing Characteristic Frequency

Bearings in service are usually pre-set with a certain radial clearance and subjected to a certain radial or axial load. The rolling element passes alternately through the load zone, and the number of loaded rollers and the bearing stiffness varies periodically. In the previous studies [12, 13], variable compliance (VC) frequencies, numerically equal to BPFO, can be observed in the frequency spectrum of healthy bearings. The outer

race fault characteristic frequency (BPFO) for a rolling bearing with a stationary outer raceway is expressed as Eq. (1).

$$BPFO = \frac{Zf_s}{2}\left(1 - \frac{D_p}{d_r}\cos\alpha\right) \tag{1}$$

where Z is the number of rollers, f_s is the shaft rotation frequency, d_r is the diameter of roller, D_p is the pitch diameter, and α is the contact angle. The type of test bearing is Timken 31308 in this study.

2.4 Experimental Conditions

To explore the effect of the internal clearance on the vibration characteristics of the TRB under different operating conditions, experiments were carried out on the TRB with different internal clearances under different rotational speeds and load states on the test rig shown in Fig. 1. The experimental condition settings and nomenclatures for different clearance conditions are given in Table 1.

Table 1. Experimental operation conditions.

| Name	Description	Radial load (kg)	Speed (1500 rpm)
PL	Preload	5,10	50%, 75%, 100%
CL 50	Clearance 50 μm	5,10	50%, 75%, 100%
CL 100	Clearance 100 μm	5,10	50%, 75%, 100%
CL 150	Clearance 150 μm	5,10	50%, 75%, 100%

3 Experimental Results and Discussion

3.1 Signal Waveform

Figure 3 shows the vibration acceleration signals of TRBs with different internal clearances under the load of 5 kg and three rotational speeds 50% (750 rpm), 75% (1125 rpm) and 100% (1500 rpm). At each speed condition, repetitive impulse features can be observed in the time domain signal waveform. Furthermore, the larger the internal clearance of TRB, the higher the vibration acceleration amplitude. These results indicate that the increase in the internal clearance of the TRB can exacerbate bearing vibration.
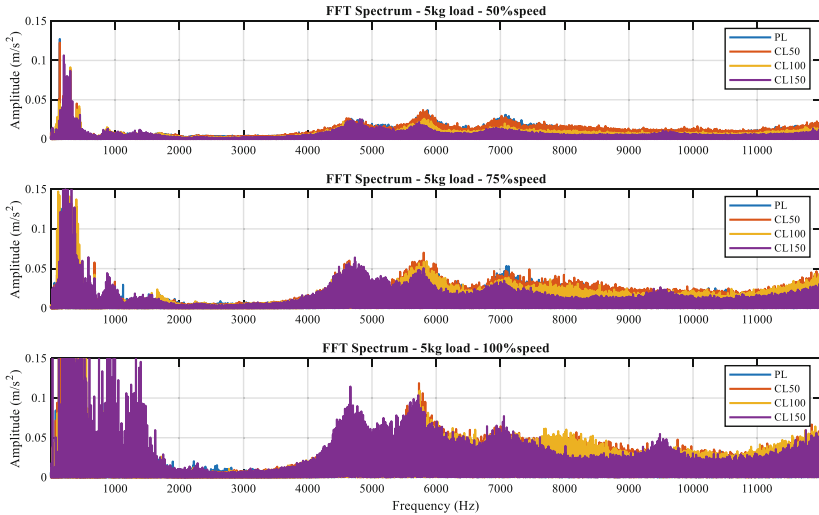
3.2 FFT Spectra

Figure 4 displays the FFT spectra of the vibration signals of TRB with different internal clearances under the load of 5 kg and three rotational speeds 50% (750 rpm), 75% (1125 rpm) and 100% (1500 rpm). It can be observed that there are frequency components

with large amplitude in the low-frequency band [0 Hz, 1500 Hz]. Figure 5 is the partial enlargement of Fig. 4. The rotational frequency and its harmonics are clearly observed in the frequency spectra, and their amplitudes increase with increasing rotational speed. In addition, BPFO (with some differences from the theoretical value indicated by the dotted line in Fig. 5) can be observed in the frequency spectra, and its amplitude increases with the increase of rotational speed. Therefore, it can be concluded that the internal clearance of TRB causes BPFO.
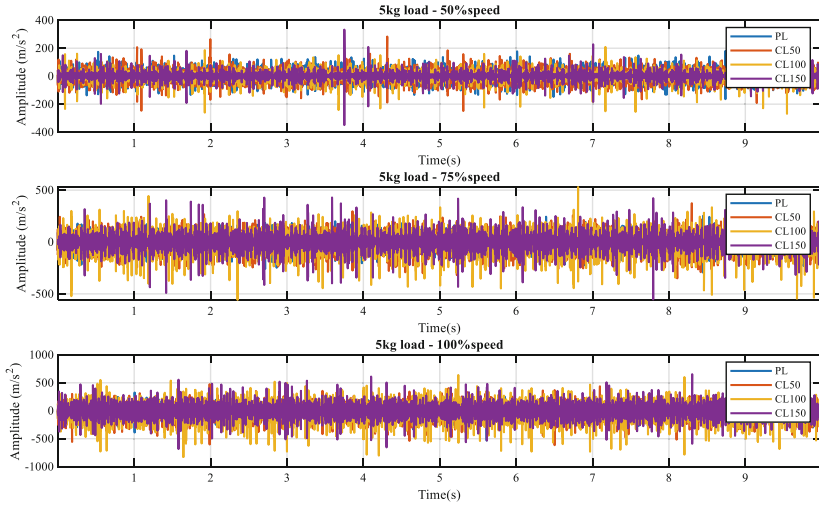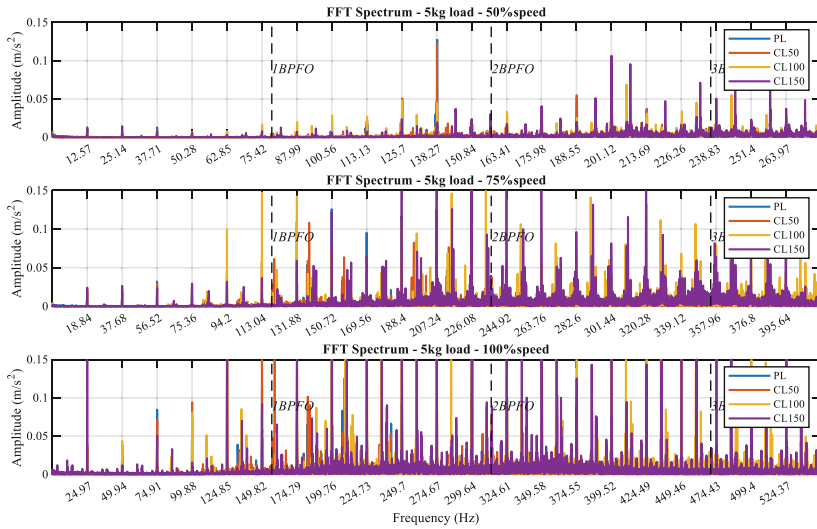

Fig. 3. Time waveforms under 5 kg load and different rotational speeds.

Fig. 4. FFT spectra under 5 kg load and different rotational speeds.

3.3 Envelope Spectra

To clearly reveal the bearing characteristic frequencies, a frequency band [3000 Hz, 6000 Hz] containing bearing-related information was selected for envelope analysis. Figure 6 shows the envelope spectra of the band-pass filtered signals of a TRB bearing with different internal clearances. Although there is a certain difference between the actual value and the theoretical value, the BPFO and its harmonics can be clearly observed. This further confirms that the internal clearance of TRB causes BPFO.

Fig. 5. Partial enlargement of FFT spectra under 5 kg load and different rotational speeds.

To explore the effect of the internal clearance on the bearing characteristic frequencies, the partial enlargement of Fig. 6 is exhibited in Fig. 7. An important finding is that when the rotational speed is fixed, as the internal clearance of the TRB increases, the actual BPFO gradually increases, that is, the difference from the theoretical value increases gradually.

The reasons for this phenomenon are discussed here. This could be explained by the fact that the friction increases while the skidding effect decreases with the clearance decreases. The premise of Eq. (1) is pure rolling and simple rolling assumptions. However, the contact behaviors of the rollers with the inner and outer raceways are related to the internal clearance. The combination of rolling and sliding occurs on the contact surface of bearing with large clearance, causing inaccurate results for Eq. (1).
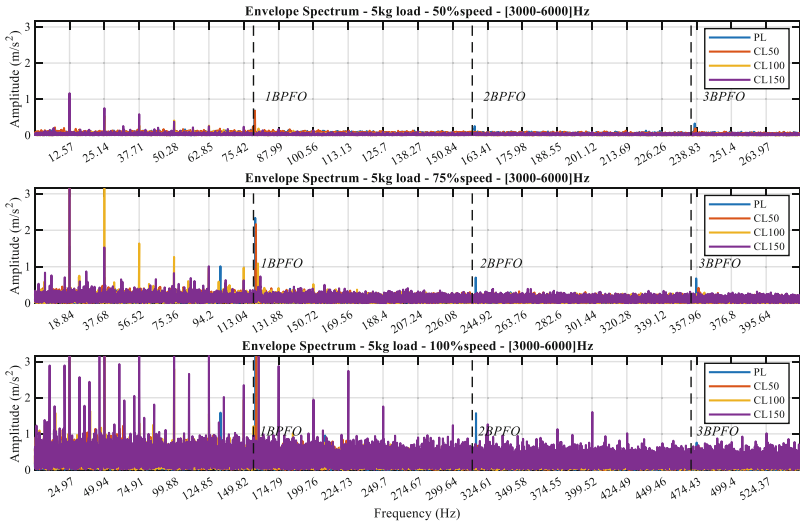
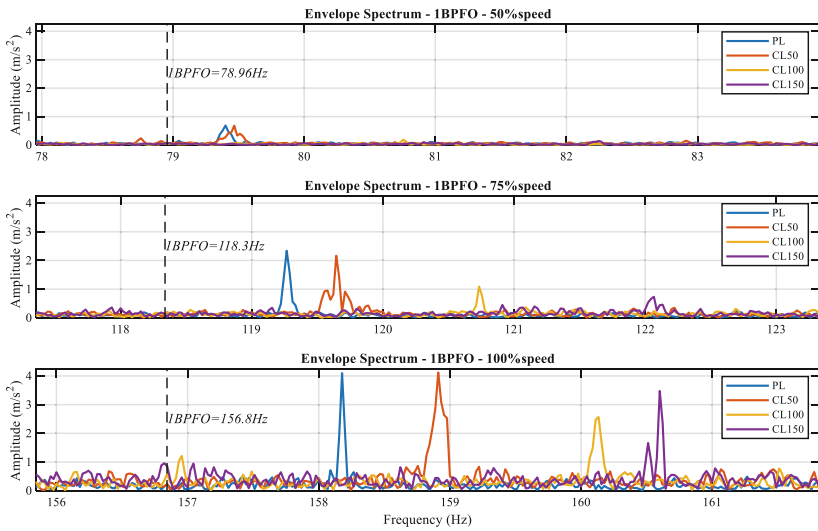**Fig. 6.** Envelope spectra under 5 kg load and different rotational speeds.

Fig. 7. Partial enlargement of envelope spectra under 5 kg load and different rotational speeds.

4 Quantitative Analysis

4.1 Influence of Clearance on RMS Value

Figure 8 gives the effect of clearance on the RMS values of acceleration responses of the tested TRB under 5 kg radial load. It can be observed that the RMS value of the bearing vibration signal increases with the increase of the internal clearance at a specific speed. For a given clearance of TRB, the RMS value shows an ascending trend when the speed

increases. The reason is that the vibration intensity of the impulse response caused by roller-race collisions not only increases as the clearance increases but is also positively related to the shaft rotational speed.

4.2 Influence of Clearance on Characteristic Frequency Shift

To quantitatively evaluate the influence of the internal clearance of TRB on BPFO, the relative error (Eq. (2)) between the theoretical result (f_t) calculated by Eq. (1) and the actual result (f_m) obtained from the measured data is proposed as an evaluation metric, as follows:

$$\Delta f = \frac{f_m - f_t}{f_t} \times 100\% \tag{2}$$

The larger the relative error, the greater the influence of the internal clearance of the TRB on the BPFO. The relative errors of the characteristic frequency shift of fault-free TRBs at different clearances and rotational speeds are calculated, as shown in Fig. 9. At 50% speed, the relative error of the BPFO increases significantly from 0.5% to 4% as the internal clearance becomes larger. A similar phenomenon can be observed at the other two speed conditions, with the range of variation decreasing as the speed increases. Another important finding is that the relative error of the BPFO decreases with increasing speed for larger clearance cases and conversely increases gradually with increasing speed for smaller clearance cases.
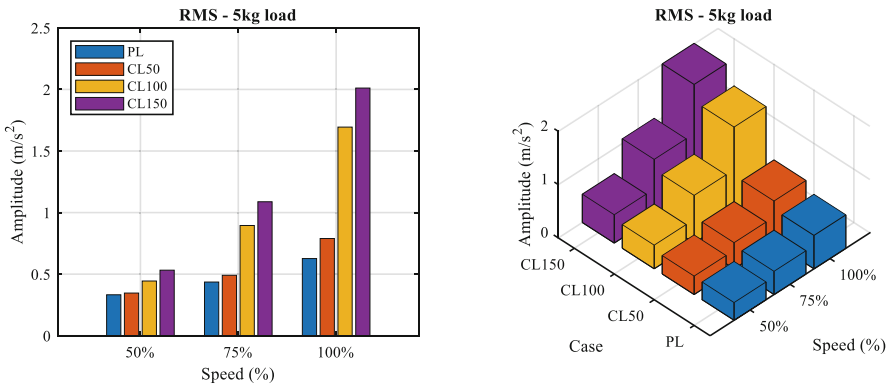

Fig. 8. RMS values of bearing vibration signals under 5 kg load.

4.3 Indicator for Clearance Size Evaluation

Based on the aforementioned analysis, the influence of the clearance on the characteristic frequency shift and RMS value of vibration signal is comprehensively explored. A two-dimensional chart was constructed to visualize the distribution differences between different clearance cases. As shown in Fig. 10, the right-pointing triangle, circle and
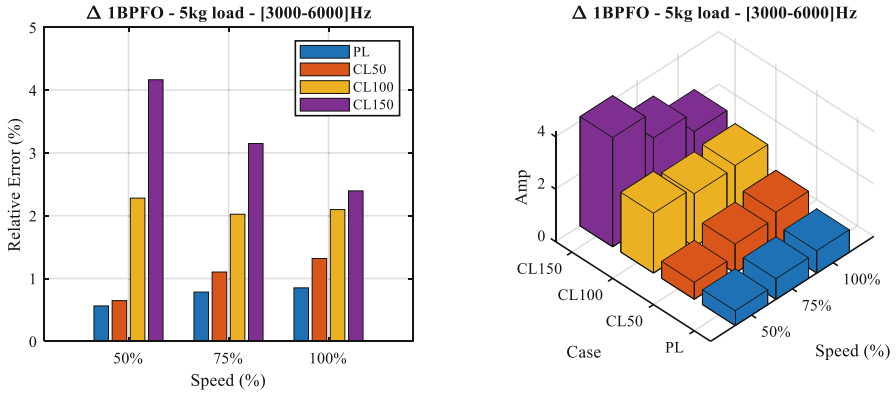
Fig. 9. Bearing characteristic frequency shift under 5 kg load.

diamond of the marker symbols indicate 50%, 75%, and 100% rotational speed respectively. Different clearance cases are denoted by four different colors, as identified in the legend.

For the smaller clearance cases (e.g., PL and CL50), the overall scatter distribution is at the bottom left of Fig. 10, with small RMS and relative errors, both of which are positively correlated with the rotational speed. For the larger clearance cases (e.g., CL100 and CL150), the scattered points all have horizontal coordinate values greater than 2%, indicating very serious slippage on bearing raceways. In addition, as the rotational speed increases, the RMS values show a more significant increasing trend compared to the smaller clearance cases. Figure 11 displays the scatter distribution of the vibration characteristics under the 10 kg radial load, showing a similar regularity to that under the 5 kg load. This means that it is possible to use these two parameters to diagnose the changes in bearing clearances.
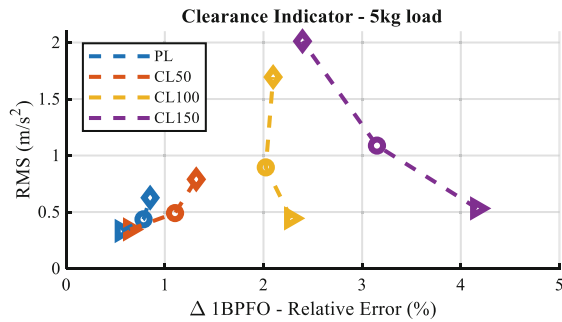
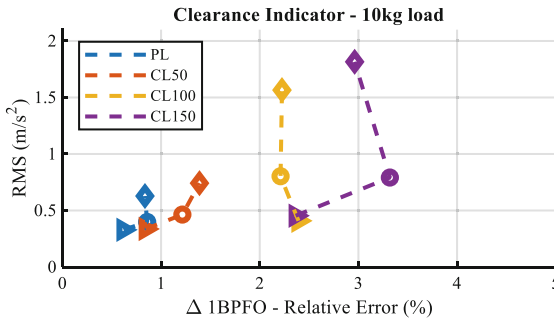**Fig. 10.** Clearance indicator under 5 kg load.

Fig. 11. Clearance indicator under 10 kg load.

5 Conclusions

A methodology has been successfully implemented to set and measure experimentally different internal clearances of a TRB. A series of experiments on a healthy TRB with different internal clearances were carried out under different operating conditions. The results show the following important findings: (1) the increase of the internal clearance leads to the increased vibration of the TRB, causing the RMS of the bearing vibration signal to increase; (2) the internal clearance of TRB will cause the BPFO and its harmonics in the FFT spectrum and envelope spectrum, and their amplitudes increase as the rotational speed increases; (3) the internal clearance of the TRB will cause the difference between the actual value of BPFO and the theoretical value, and the actual BPFO increases with the increase of the internal clearance. Therefore, the deviation between the measured value and the theoretical value of BPFO combined with the RMS value of the bearing vibration signal can be used as an indicator of the TRB clearance condition.

References

1. Chen, B., Cheng, Y., Zhang, W., Gu, F.: Investigations on improved Gini indices for bearing fault feature characterization and condition monitoring. Mech. Syst. Signal Process. **176**, 109165 (2022)
2. Randall, R.B., Antoni, J.: Rolling element bearing diagnostics-a tutorial. Mech. Syst. Signal Process. **25**, 485–520 (2011)
3. Chen, B., Cheng, Y., Zhang, W., Gu, F., Mei, G.: Optimal frequency band selection using blind and targeted features for spectral coherence-based bearing diagnostics: a comparative study. ISA Trans. **127**, 395–414 (2021)
4. Tian, X., Xi Gu, J., Rehab, I., Abdalla, G.M., Gu, F., Ball, A.D.: A robust detector for rolling element bearing condition monitoring based on the modulation signal bispectrum and its performance evaluation against the Kurtogram. Mech. Syst. Signal Process. **100**, 167–187 (2018)
5. Smith, W.A., Borghesani, P., Ni, Q., Wang, K., Peng, Z.: Optimal demodulation-band selection for envelope-based diagnostics: a comparative study of traditional and novel tools. Mech. Syst. Signal Process. **134**, 106303 (2019)
6. Chen, B., Cheng, Y., Zhang, W., Gu, F.: Enhanced bearing fault diagnosis using integral envelope spectrum from spectral coherence normalized with feature energy. Meas. J. Int. Meas. Confed. **189**, 110448 (2022)

7. Hu, L., Xu, Y., Gu, F., He, J., Hu, N., Ball, A.: Autocorrelation ensemble average of larger amplitude impact transients for the fault diagnosis of rolling element bearings. Energies **12**, 4740 (2019)
8. Luo, P., Hu, N., Zhang, L., Shen, J., Cheng, Z.: Improved phase space warping method for degradation tracking of rotating machinery under variable working conditions. Mech. Syst. Signal Process. **157**, 107696 (2021)
9. Zhang, W., Shi, P., Li, M., Han, D.: A novel stochastic resonance model based on bistable stochastic pooling network and its application. Chaos Solitons Fractals **145**, 110800 (2021)
10. Tiwari, M., Gupta, K., Prakash, O.: Effect of radial internal clearance of a ball bearing on the dynamics of a balanced horizontal rotor. J. Sound Vib. **238**, 723–756 (2000)
11. Harsha, S.P.: Nonlinear dynamic response of a balanced rotor supported by rolling element bearings due to radial internal clearance effect. Mech. Mach. Theory. **41**, 688–706 (2006)
12. Wang, J., Xu, M., Zhang, C., Huang, B., Gu, F.: Online bearing clearance monitoring based on an accurate vibration analysis. Energies **13**, 389 (2020)
13. Xu, M., Feng, G., He, Q., Gu, F., Ball, A.: Vibration characteristics of rolling element bearings with different radial clearances for condition monitoring of wind turbine. Appl. Sci. **10**, 4731 (2020)
14. Xu, M., Han, Y., Sun, X., Shao, Y., Gu, F., Ball, A.D.: Vibration characteristics and condition monitoring of internal radial clearance within a ball bearing in a gear-shaft-bearing system. Mech. Syst. Signal Process. **165**, 108280 (2022)
15. Yang, L., Xu, T., Xu, H., Wu, Y.: Mechanical behavior of double-row tapered roller bearing under combined external loads and angular misalignment. Int. J. Mech. Sci. **142–143**, 561–574 (2018)